

Intramembrane Signaling Mediated by Hydrogen-Bonding of Water and Carboxyl Groups in Bacteriorhodopsin and Rhodopsin¹

Akio Maeda,^{*2} Hideki Kandori,^{*} Yoichi Yamazaki,^{*} Shoko Nishimura,^{*} Minoru Hatanaka,^{*} Young-Shin Chon,^{*} Jun Sasaki,^{*,3} Richard Needleman,[†] and Janos K. Lanyi[‡]

^{*}Department of Biophysics, Graduate School of Science, Kyoto University, Kyoto 606-01; [†]Department of Biochemistry, Wayne State University School of Medicine, Detroit, MI 48201, USA; and [‡]Department of Physiology and Biophysics, University of California, Irvine, CA 92717, USA

Received for publication, November 22, 1996

The light-induced mechanism for proton pumping of bacteriorhodopsin was studied by Fourier transform infrared spectroscopy of the discrete sequential intermediate states, L, M, and N. Attention is focused on L in the early microsecond time range, as a transition state in which the Schiff base forms strong H-bonding with a water molecule coordinated with Asp85. This structure leads to transfer of the Schiff base proton to Asp85 in the L-to-M process, which then triggers proton release from Glu204 to the extracellular surface. H-bonding of Arg82 and water molecules are involved in this process. Chloride can replace Asp85 in the D85T mutant, and this anion will be then transported instead of a proton. In L, structural perturbations are induced also around Asp96, through a string of H-bonding mediated by internal water molecules and peptide carbonyls in helices B and C, and Trp182 in helix F. These may cause the structural changes that occur later in the M-to-N process. Similar interactions, through internal water molecules and the peptide bonds in helices B and C, take place in bovine rhodopsin. They transduce changes across the membrane from the Schiff base to the cytoplasmic surface, where the activation of the transducin occurs.

Key words: bacteriorhodopsin, FT-IR, halorhodopsin, proton pathway, rhodopsin.

Bacteriorhodopsin and its photointermediate

Bacteriorhodopsin is a transmembrane heptahelical protein (molecular weight of about 26,000) with a retinal bound to the ϵ -amino group of Lys216 *via* a protonated Schiff base (Fig. 1). The protein can conceptually be divided into the extracellular and cytoplasmic domains by the polyene chain of the retinal that lies nearly parallel with the two membrane surfaces. Polar amino acid residues are more abundant in the extracellular domain, while the cytoplasmic domain is largely composed of hydrophobic residues (1). The retinal chromophore is a mixture of all-*trans* and 13-*cis*, 15-*syn* isomers in the dark. Illumination converts all of the chromophore to the all-*trans* form, the "light-adaptation process" (2).

Only the all-*trans* bacteriorhodopsin in the unphotolyzed state (BR) transports protons in the reaction cycle induced by light absorption. The intermediates named J, K, L, M, N, and O in this order arise from the light-induced isomerization to the 13-*cis*, 15-*trans* state (Fig. 2). The retinal returns to the all-*trans* state in O, and then restores

the initial state, BR. The cycle is completed in less than 10 ms. M is the only intermediate with an unprotonated Schiff base. Proton moves from the Schiff base to Asp85 in the L-to-M process and another proton moves from Asp96 to the Schiff base in the M-to-N process (3-6, reviews).

It is more advantageous to study bacteriorhodopsin than other functional proteins because these discrete intermediate states can be distinguished over a picosecond to millisecond time range. Structural analysis of these intermediates by spectroscopic methods can reveal the chemical processes for the functions. K is present up to nanosecond range, L is in the early microsecond range, M occurs up to several milliseconds and N and O arise directly afterward. All of these states are in equilibrium with each other except for two M species at neutral pH, M₁ and M₂ (4). This irreversible step prevents the reverse flow of protons. Difference spectra upon formation of most of these intermediates were recorded by time-resolved spectroscopy and also in a conventional spectrometer at 80 K for K, 170 K for L, 230 K for M, and 274 K for N (6). The spectrum of O can only be obtained by time-resolved manner (7). These intermediates were defined first by visible spectra, but more unequivocal assignments can be achieved by FT-IR spectra (6).

FT-IR spectroscopy

FT-IR (Fourier transform infrared) studies have revealed the protonation states of carboxylic acid residues, H-bonding changes in water, peptide carbonyls, and others

¹ This work was supported by Grants-in-Aid from the Ministry of Education, Science, Sports and Culture of Japan to AM (06404082, 08268225) and HK (07839003).

² To whom correspondence should be addressed. E-mail: maeda@photo2.biophys.kyoto-u.ac.jp

³ Present address: Department of Structural Biology, Biomolecular Engineering Research Institute, 6-2-3, Furuedai, Suita, Osaka 565. Abbreviations: BR, all-*trans* bacteriorhodopsin in the unphotolyzed state; HOOP, hydrogen out-of plane.

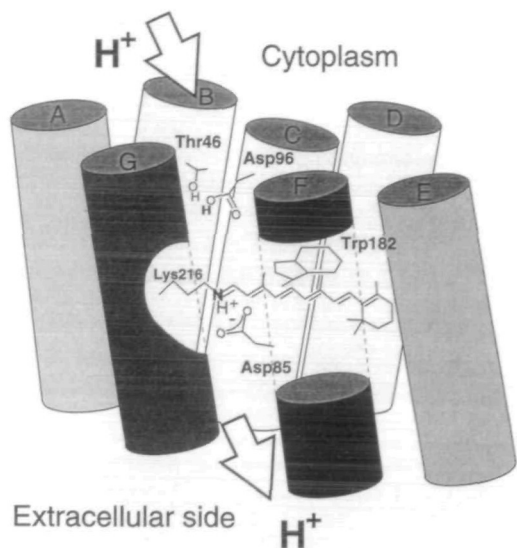


Fig. 1. Seven helices of bacteriorhodopsin with important residues for the function.

(6). These residues have important roles in the functions. Chemical bonds involved in the function of proteins, such as O-H, N-H, and C=O, are polar in nature, and undergo changes in polarity and H-bonding during reactions. Such changes are favorably picked up by difference FT-IR spectroscopy as intensity and frequency changes, as shown for the *L minus BR* spectrum as an example (Fig. 3). The large shifts of the frequency that depend on the protonated states of carboxylic acids and the Schiff base in the consecutive intermediates allow depiction of the proton transfer pathways. Diffraction studies, with cryoelectron microscopy, of the tertiary structure of the unphotolyzed state of bacteriorhodopsin (8) are useful to supplement the knowledge of the intermediates provided by those FT-IR studies. The results at 3 Å resolution that will be published in near future (9) must be useful for better understandings.

One of the restrictions in recording FT-IR spectra is that the water content of the samples has to be reduced but to an extent that does not cause kinetic defects for the intermediates concerned. Usually, we do it by adding a controlled amount of water to air-dried films and examining the absorbance around $3,300\text{ cm}^{-1}$ of the O-H stretching vibrations of water. For the recordings of L and M, the water content is adjusted to about 50%. Under these

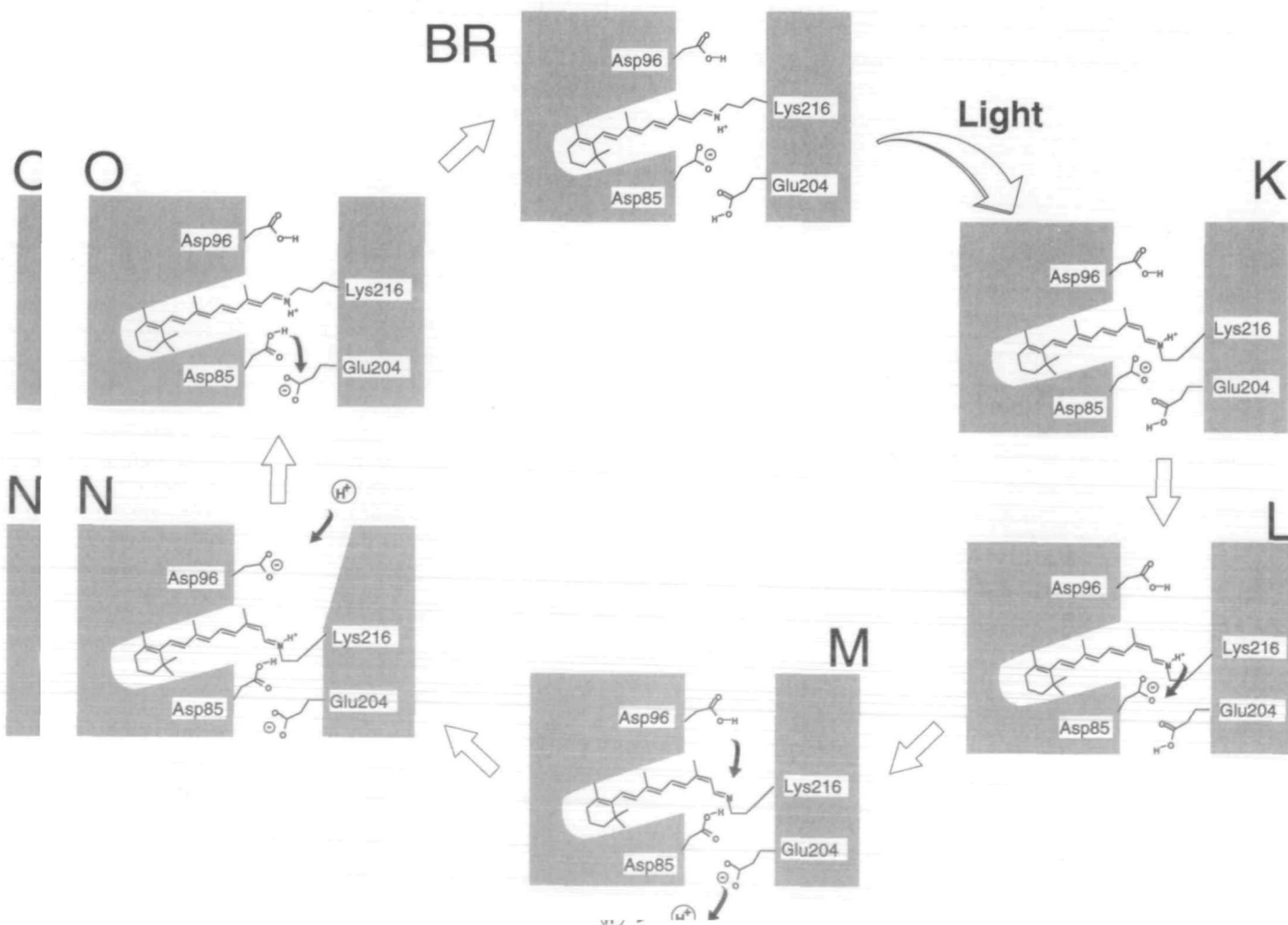


Fig. 2. Photointermediates of bacteriorhodopsin and their structures. See the details for the text.

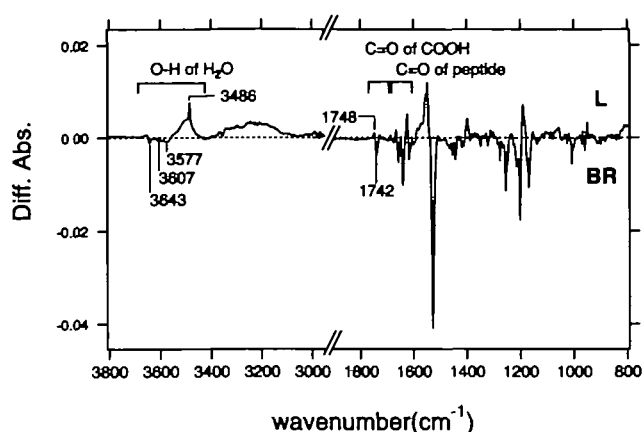


Fig. 3. *L* minus BR spectrum of bacteriorhodopsin.

conditions, we obtained the same kinetic behavior for *L* in the film as that in the suspensions at room temperature. For the recordings of the spectral changes in *N* and *O*, we have to add water to more than 70% (10), because the decay of the precedent intermediate *M* is slowed under the conditions used for *L* and *M*.

L as a transition state

The proton of the Schiff base is transferred to Asp85 in the *L*-to-*M* process (Fig. 2). The Schiff base N-H of BR is directed toward Asp85 in the extracellular domain (3), and connects to it with very weak H-bonding interaction (11). If restriction by the protein were absent, the photoisomerization of the retinal would force the direction of the Schiff base N-H to change to the opposite side from Asp85. However, the proton transfer from the Schiff base to Asp85 in the *L*-to-*M* conversion requires that the Schiff base N-H remains connected to Asp85 even in *L*. This concept has induced us to study the structure of *L*, as the most crucial and intriguing state for the subsequent reactions.

For the proton transfer from the Schiff base to Asp85, the most immediate reaction after *L*, the interaction of the protonated Schiff base with Asp85 is necessary. Indeed, the protonated Schiff base forms first strong H-bonding in *L* as reflected in the N-H in-plane bending vibration of the Schiff base at higher frequency than in either BR or K (12). Distortion of the retinal close to the Schiff base is revealed by the smaller intensity of the in-plane bending vibrational band of C₁₅-H in *L* than *N* (10). This is the structure that allows the Schiff base N-H to connect to Asp85 in *L*. Distortion close to the Schiff base has already begun in *K*, as revealed by the presence of C₁₅-hydrogen out-of-plane (HOOP) bands at 960 and 985 cm⁻¹ (13). Among them, the 960-cm⁻¹ band prevails in *K*. In the 10 ns time range this state changes to the other *K*-like state, *KL*, in which the 985-cm⁻¹ band is more intense (14). The corresponding band of C₁₅-HOOP is further shifted to higher frequency in *L* (12).

Structural changes of water were disclosed by difference FT-IR spectroscopy upon the photoreaction (15). A water molecule with its O-H stretching vibration at 3,643 cm⁻¹ (Fig. 3) was found complexed with Asp85 (11). Upon *L* formation, this O-H forms stronger H-bonding with Asp212, which is located close to Asp85 (16). This complex

structure includes the water molecule that is linked to Asp85, Asp212, and the Schiff base, and induces distortion in the retinal. The most important contribution in this structure must be the strong H-bonding of the protonated Schiff base. The intervening water molecule may be important also for the separation of the positive charge of the protonated Schiff base and the negative charge on Asp85 (17). Such a distorted structure would induce the proton transfer by decreasing the p*K*_a value of the Schiff base (18, 19). Transfer of its proton to Asp85 causes the neutralization of these electric charges, and inevitably releases the distorted structure around the Schiff base. It results in relaxed structure in *M*, and even in *N* with a reprotonated Schiff base. Thus, the Schiff base no more drives proton transfer reactions in *M* and *N*, and the large protein changes inherent for *N* have to be induced by continued structural changes that already started in *L*. Such an *L*-to-*M* process cannot be reversed, and comprises part of the switch for unidirectional proton pumping (4).

Molecular dynamic calculations based on the old Henderson model (1) by Humphrey *et al.* (20) have proposed a possible structure for *L*, in which the Schiff base N-H in a distorted chromophore points parallel to the membrane plane and is connected to Asp85 through a water molecule. Upon formation of *M*, the unprotonated Schiff base nitrogen turns its lone pair to the side opposite from Asp85 (21).

Structure around the Schiff base and chloride transport

The negative charge of Asp85 has the role to compensate the positive charge of the Schiff base. Its replacement by neutral amino acids, like threonine or asparagine, causes an imbalance of electric charges around the Schiff base. Consequently, the absorption band in the visible spectrum is shifted to the red, and proton pumping activity is abolished due to lack of an acceptor. Photoreaction produces an *L*-like state but the distorted structure of *L* is lost due to the absence of interaction with the negative charge of Asp85 (11). Addition of chloride restores the absorption spectrum to its original shape, and a normal *L* forms (22). In the case of D85T mutant, chloride transport was observed in the same direction as halorhodopsin (23), although no similar activity was detected in the D85N mutant. This may be related to the fact that the corresponding residue in the chloride pump, halorhodopsin, is threonine (24). Thus, the replacement of a single residue at the active center changes the proton pump to a chloride pump. If the counterion is a fixed anion, bacteriorhodopsin works as the proton pump, and if the counterion is a mobile chloride, it is transported by this protein. Analysis of the FT-IR spectra shows that a water molecule is present between the Schiff base and the bound chloride, that undergoes H-bonding change upon *L* formation (22), as the water molecule between the Schiff base and Asp85 in the wild type.

The mechanism of chloride-transport in bacteriorhodopsin can be depicted on the basis of proposed mechanism on chloride transport in halorhodopsin (25, 26). Chloride is fixed to the Schiff base with the aid of Arg82. Upon light-dependent isomerization of the retinal, the chloride is brought to the cytoplasmic side, where no complementary positive charge of Arg82 is present, by complexing with the Schiff base and eventually released into the cytoplasmic

half (27). Reisomerization to the all-*trans* form occurs in this chloride-free state (25). The binding of another chloride from the extracellular medium then resets the system, and completes the cycle for chloride transport.

Long range interaction between Asp85 and Asp96 in L

Perturbation around Asp96 (28, 29) is the next issue in L. This may relate to deprotonation of this residue in N at the remote site from Asp85 on the cytoplasmic side. The C=O stretch of Asp96 shifts from 1,742 to 1,748 cm^{-1} (Fig. 3) by rendering H-bonding weaker upon L formation. T46V makes this H-bonding further weaker (30). This indicates close interaction of Thr46 with Asp96. Flash-induced absorbance changes in the microsecond time range indicate that T46V accelerates the proton transfer from the Schiff base to Asp85, and the normal rate for the proton transfer is restored with the additional D96N mutation in T46V/D96N (30). These results strongly imply long range interaction between the regions of Asp96 and Asp85. The question of what the structural connection between these two residues must be asked.

FT-IR spectra can detect changes in H-bonding of the peptide C=O (amide I). The amide I bands at 1,618 (–) and 1,625 (+) cm^{-1} in the L *minus* BR spectrum were identified as the peptide C=O of valine residues by their specific ^{13}C labeling (31). In general, peptide carbonyl bands cannot be identified by mutations, because they are in principle not affected by changes in the side chain. Indeed, site directed isotope labeling was needed for the assignment of a particular band to the peptide carbonyl of Tyr185 in N (32). Though the V49A mutation has no influence, in V49M the intensities of these bands are decreased. These peptide C=O bands are ascribed to the carbonyl of Val49 (31).

The L *minus* BR spectrum exhibits O–H stretch bands for water at 3,643, 3,607, and 3,577 cm^{-1} for BR (Fig. 3). The number of water molecules involved is one or a few for each band, judging from the molar extinction (15, 30, 31). Among them, the 3,643 cm^{-1} band is attributed to a water molecule present close to the unprotonated Asp85 because it is absent in D85N (11). The 3,607 cm^{-1} band is ascribed to a water molecule close to Asp96 because it is absent in D96N (30), and the 3,577 cm^{-1} band to the water molecule close to the peptide carbonyl of Val49 because in V49M it is absent, together with decrease of its carbonyl intensity (31). The T46V mutation abolishes the two bands at 3,607 and 3,577 cm^{-1} together (30), suggesting that Thr46 is located at a key position for these two water molecules. The V49M and V49A mutations also affect the intensity of the water O–H stretch at 3,643 cm^{-1} (31).

These results are explained in Fig. 4. The peptide C=O of Val49 forms H-bonding with a water O–H, and this water molecule is further connected to the water molecule complexed to Asp85. On the basis of the fact that V49A and V49M also influence the C=O of Asp96 in the opposite, cytoplasmic side, we can depict a structure with H-bonding interactions of the side chain of Thr46 with the C=O of Asp96 in the one hand, and the peptide N–H of Val49 in the other. Water molecules intervene in these H-bonds. This is the structural basis for the key role of the peptide bond of Val49 in long range interaction from Asp96 to Asp85 containing water. All of these water molecules form stronger H-bonding upon L formation as evidenced by shifts of the O–H stretch toward lower frequency, suggest-

ing their important structural role (31).

Transfer of the proton of the Schiff base to Asp85 upon conversion to M collapses this complex around the site close to Asp85. Namely, the strong H-bonding of the Schiff base N–H with the protein is abolished, and the nitrogen of the unprotonated Schiff base directs its lone pair to the side opposite from Asp85. Distortion in the retinal is thus abolished. This can be one of the switch reactions in the unidirectional proton pumping (4, 33). Molecular dynamics calculations show that one of the water molecules is present close to Asp85 in L moves far from it and makes some connection with residues in the cytoplasmic side (21). Instead of weakened H-bonding of the water molecule, the C=O of Asp96 acquires strong H-bonding (34). These would be involved in the mechanism for the deprotonation of Asp96 and the reprotonation of the Schiff base in the M-to-N conversion.

Interaction of Trp182 in helix F with the retinal

L shows also increase in intensity of the N–H stretching vibrational band at 3,486 cm^{-1} (Fig. 3). This band is shifted in [indole- ^{15}N]-labeled bacteriorhodopsin (35). It is assigned to Trp182, because this band vanishes in W182F (36). The indole of Trp182 is interacting with the 9-methyl group of the retinal because the N–H stretching vibration of this band decreases in intensity if the retinal is replaced by 9-desmethyl retinal. The increase in the intensity of this band must be the result of electric interaction of the indole with the retinal through the 9-methyl group. This interaction favors the proton transfer from the Schiff base to Asp85 in the L-to-M process (36).

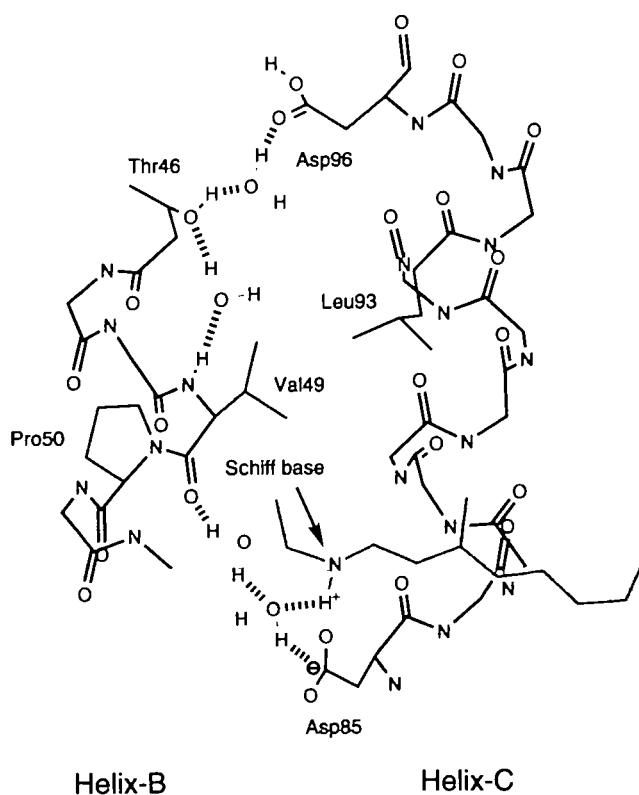


Fig. 4. H-bonding network from Asp85 to Asp96. Water molecules and peptide carbonyls are emphasized.

The interaction is seen in **L** but not in **M** and **N** (35). Nevertheless, large conformation distortion of **N** is induced in helix F (37), in which Trp182 is included. This suggests that the origin of the conformation distortion in **N** has already begun in **L**. Molecular dynamics calculation of **M** suggests a distorted structure for Trp182 (21).

H-bonding network in the extracellular domain

The next topic is the H-bonding network of water from Asp85 to Glu204, the proton releasing residue at the extracellular surface in **M** (Fig. 2). The proton transferred from the Schiff base to Asp85 remains at this residue. Therefore, the proton release to the covalently attached dye on the extracellular surface, observed with a slight delay to the protonation of Asp85, must occur from another site (38). Glu204 has been proposed to be this site as revealed by a markedly delayed proton release in E204Q, and by normal releasing kinetics in E204D (39). The mutants of Arg82 also exhibit a similar delay in the proton release (40). However, Arg82 is not necessary for proton release (41, 42). Rather its positive charge is proposed to enhance the proton release from Glu204 when the Schiff base is uncharged. Under these conditions Arg82 allows either Asp85 or Glu204 to become deprotonated (42). FT-IR studies have shown the deprotonation of Glu204 in the **L**-to-**M** process (39) for the proton release, though the smaller intensity of this band in comparison with other carboxylic acid residues implicates an H-bonding network that includes this residue. A small water O-H band at $3,625\text{ cm}^{-1}$ in the **M** minus **BR** spectra is absent in the mutants of Glu204 (39) and Arg82 (43). This indicates the presence of water molecules in the Arg82-Glu204 region and that they undergo structural changes upon **M** formation, or may even deprotonate.

In a simple model based on electrostatic interactions, the protonation of Asp85 results in the deprotonation of Glu204, which in turn stabilizes the protonated state of Asp85. This blocks the reverse flow of the proton, ensuring the one-way proton transport (33). This would explain the effects of Arg82 on the proton release. However, it is possible that the guanido N-H of Arg82 may mediate this interaction through H-bonding between Asp85 and Glu204 (43).

The water molecule close to Asp85 exhibits an O-H stretch at $3,643\text{ cm}^{-1}$ in **BR** (Fig. 3). This band is shifted by $5\text{--}7\text{ cm}^{-1}$ toward lower frequency in the mutants of Arg82 and Glu204, suggesting that an H-bonding system is connected to the water molecule close to Asp85 in **BR**. In contrast, the water band at $3,671\text{ cm}^{-1}$ in **M** is neither affected by the mutation of Arg82 nor Glu204. This water molecule must be located in the cytoplasmic side of the membrane (43).

Protein changes in the last photocycle steps

N is formed from **M** by proton transfer from Asp96 to the Schiff base, resulting in the reprotonation of the Schiff base and deprotonation of Asp96 (Fig. 2). This is first suggested by kinetic studies by use of D96N (44), and then confirmed by the difference FT-IR spectrum upon **N** formation (10). The protonated Asp85 is in a more polar environment in **N** than **M**, as evident from the shift of the C=O stretch of Asp85 from $1,762$ to $1,755\text{ cm}^{-1}$. Stronger H-bonding formation also occurs in several peptide carbonyls. The

same environmental changes of the carbonyls of Asp85 and the peptide bonds are induced even without reprotonation of the Schiff base in a state named **M_N**, in which the chromophore is like an **M**-like state but the protein part is already in the **N** state (45). The structure of the chromophore around the protonated Schiff base is already in a relaxed state in **N** in contrast to the distorted structure in **L** (10), and the Schiff base is no longer involved in inducing structural changes. The perturbation of Asp85 is probably mediated by the H-bonding string from Asp96, because azide-mediated reprotonation of the Schiff base is dependent on the residue at position 96 (46). Diffraction studies on **N** indicate the tilting of the cytoplasmic half of helix F, as in **M_N** (37). This seems to be already triggered in **L**, because Trp182 in the cytoplasmic side of the helix F interacts with the 9-methyl group of the retinal (36).

The next event in the proton pumping process is the reprotonation of Asp96 through multiple residues from the cytoplasmic surface (47, 48). The reisomerization of the retinal to the all-*trans* form is a prerequisite for the restoration of the original state. The all-*trans* intermediate thus formed is **O**. The chromophore contains a twisted chain close to the Schiff base, and forms strong H-bonding (49), probably with a residue other than the protonated Asp85 because the C=O stretching frequency of Asp85 remains unchanged in the **N**-to-**O** process (7). It could be a system including Tyr185 because Y185F shows a very long life time of **O** and abolishes the twists around the Schiff base (7). Such structure then induces the proton transfer from Asp85 to Glu204 as the final resetting reaction (50).

Common mechanism in rhodopsin

The results described above have shown the structural roles of internal water molecules and peptide bonds in the function of bacteriorhodopsin. It is intriguing to explore the possibility of a similar mechanism in a related protein that is a G-protein coupled receptor. Rhodopsin as the vision receptor is the most characteristic among these. It is also transmembrane heptahelical protein, and contains 11-*cis* retinal attached to Lys296 with the protonated Schiff base (Fig. 5). A series of intermediates is produced by the light-dependent isomerization to the all-*trans* form. Meta-rhodopsin II (**Meta II**) is formed from metarhodopsin I (**Meta I**) with proton transfer from the Schiff base to Glu113 (51). Its formation is accompanied by the uptake of a proton through Glu134 on the cytoplasmic surface, as a reflection of a pH-dependent equilibrium with its precursor, **Meta I** (52). Such protonated **Meta II** is responsible for the GTP-GDP exchange in the α -subunit of G-protein, transducin (**T α**) (53). The **T α** -binding GTP then activates cyclic GMP-phosphodiesterase, finally leading to changes in electric properties of the plasma membrane of the rod outer segments of retinae.

Difference FT-IR spectra were obtained for the late intermediates, **Meta I** and **Meta II**, as well as earlier ones, bathorhodopsin (**Batho**) and lumirhodopsin (**Lumi**). One of the characteristic features in the chromophore of **Batho** is twists in the polyene chain, as reflected by strong HOOP bands in the resonance Raman spectrum and the presence of perturbation of a negative charge close to C₁₂-H, as reflected by the uncoupled C₁₂-HOOP at 921 cm^{-1} (54). The same bands were detected also in FT-IR spectra (55). We have further characterized the HOOP bands of **Lumi**, and

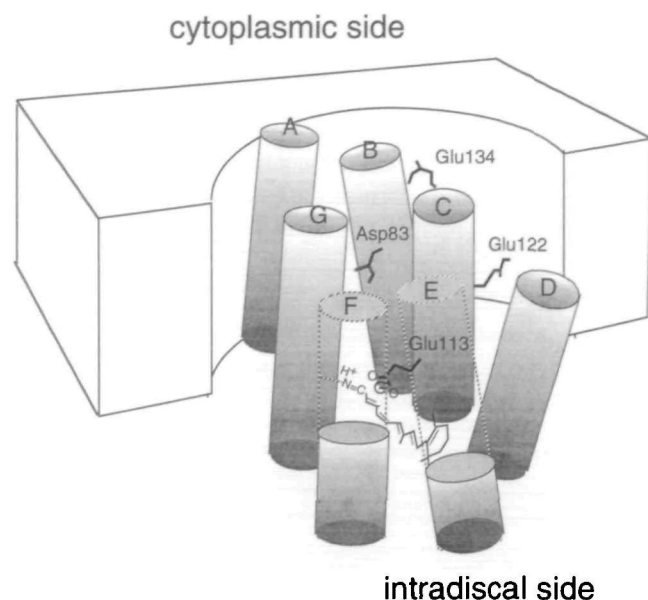


Fig. 5. Seven helices of bovine rhodopsin with important residues for the function.

Meta I. The perturbation of the negative charge is lost in **Lumi** and **Meta I**, as envisaged from the presence of the coupled band of C_{11} -HOOP and C_{12} -HOOP at 950 cm^{-1} . Although **Lumi** and **Meta I** resemble each other, the 886 cm^{-1} band of C_{14} -HOOP in the C_{12} -D derivative of **Meta I** is not observed in **Lumi**. Since the C_{14} -HOOP band gains intensity influenced by the neighboring polar Schiff base N-H, its absence must be the result of the twist of the retinal around the Schiff base. Thus, **Lumi** is distorted around the Schiff base but **Meta I** is not (56). This is analogous to **L** of bacteriorhodopsin as the transitional state with a distorted chromophore. The corresponding lumirhodopsin and mesorhodopsin of octopus rhodopsin are also shown to have distorted Schiff base linkages (57). Studies on invertebrate rhodopsin are also useful to explore the role of the interaction of the Schiff base with the counterion. There is no such counterion residue in octopus rhodopsin. The Schiff base is complexed with a water molecule after the photoreaction, and these water and peptide carbonyls are involved in stabilization of the protonated Schiff base in acid-metarhodopsin (57), which is supposed to be the signaling state to the specific G-protein, Gq (58).

H-bonding changes in water molecules were examined for these intermediates. Stronger H-bonding forms in the photochemical reactions to **Batho** (59), **Lumi**, and **Meta I** (60). The structural changes of a water molecule were suggested to occur around the Schiff base upon **Batho** formation (59). For air-dried rhodopsin film with water content less than 15%, the conversion from **Lumi** to **Meta I** becomes extremely slow and **Meta II** does not appear (61). We used this system to examine the relation of internal water molecules in the membrane to the process from **Meta I** to **Meta II**. Under these conditions, perturbation of the carbonyl of Glu122 does not occur, and the relaxation of the twist in the Schiff base region of the chromophore typical for **Meta I** is also absent, **Meta I** exhibiting features similar to those of **Lumi** (61). Thus, the blockage of the relaxation around the Schiff base with the

depletion of water inhibits the structural changes in the intramembrane residues around Glu122, and the eventual conversion to **Meta II**, which requires the structural changes in the cytoplasmic side. The transmembrane pathways of H-bonding strings through helices B and C are thus implicated to be common for bacteriorhodopsin and rhodopsin.

Activation of transducin occurs on the surface of **Meta II**. It is known that the equilibrium between **Meta I** and **Meta II** shifts to **Meta II** when transducin is present. If GTP binds to the α -subunit, the equilibrium reverses with an accompanying release of $T\alpha$. We used this system to detect the changes upon binding of $T\alpha$ to **Meta II** (62). No changes in internal carboxylic acids like Asp83, Glu122, and Glu113 occur. Only the protonation of a small fraction of carboxylate, presumably Glu134, was observed. Strengthening of H-bonding of one or a few peptide carbonyls is the most significant change.

REFERENCES

- Henderson, R., Baldwin, J.M., Ceska, T.A., Zemlin, F., Beckman, E., and Downing, K.H. (1990) Model for the structure of bacteriorhodopsin based on high-resolution electron cryomicroscopy. *J. Mol. Biol.* **213**, 899-929
- Harbison, G.S., Smith, S.O., Pardo, J.A., Winkel, C., Lugtenburg, J., Herzfeld, J., Mathies, R., and Griffin, R.G. (1984) Dark-adapted bacteriorhodopsin contain 13-*cis*, 15-*syn* and all-*trans*, 15-*anti* retinal Schiff bases. *Proc. Natl. Acad. Sci. USA* **81**, 1706-1709
- Mathies, R.A., Lin, S.W., Ames, J.B., and Pollard, W.T. (1991) From femtoseconds to biology: mechanism of bacteriorhodopsin's light-driven proton pump. *Annu. Rev. Biophys. Biophys. Chem.* **20**, 491-518
- Lanyi, J.K. (1993) Proton translocation mechanism and energetics in the light-driven proton pump bacteriorhodopsin. *Biochim. Biophys. Acta* **1183**, 241-261
- Lanyi, J.K. and Váró, G. (1996) The photocycle of bacteriorhodopsin. *Israel J. Chem.* **35**, 365-385
- Maeda, A. (1996) Application of FT-IR spectroscopy to the structural study on the function of bacteriorhodopsin. *Israel J. Chem.* **35**, 387-400
- Bousché, O., Sonar, S., Krebs, M.P., Khorana, H.G., and Rothschild, K.J. (1992) Time-resolved Fourier transform infrared spectroscopy of the bacteriorhodopsin mutant Tyr185→Phe: Asp-96 reprotonates during O formation; Asp-85 and Asp-212 deprotonate during O-decay. *Photochem. Photobiol.* **58**, 1085-1096
- Grigorieff, N., Ceska, T.A., Downing, K.H., Baldwin, J.M., and Henderson, R. (1996) Electron-crystallographic refinement of the structure of bacteriorhodopsin. *J. Mol. Biol.* **259**, 393-421
- Mitsuoka, K., Miyazawa, A., Vassilyev, D., Kidera, A., Matsuhashima, A., Murata, K., Hirai, K., Fujiyoshi, Y., and Kimura, Y. (1995) Three dimensional map of bacteriorhodopsin at 3.0 Å resolution. *Abstracts of 7th International Conference on Retinal Protein (Zichron Yaakov, Israel)* **2**
- Pfefferlé, J.-M., Maeda, A., Sasaki, J., and Yoshizawa, T. (1991) Fourier transform infrared study of the N intermediate of bacteriorhodopsin. *Biochemistry* **30**, 6548-6556
- Maeda, A., Sasaki, J., Yamazaki, Y., Needleman, R., and Lanyi, J.K. (1994) Interaction of aspartate-85 with a water molecule and the protonated Schiff base in the L intermediate of bacteriorhodopsin: A Fourier transform infrared spectroscopic study. *Biochemistry* **33**, 1713-1717
- Maeda, A., Sasaki, J., Pfefferlé, J.-M., Shichida, Y., and Yoshizawa, T. (1991) Fourier transform infrared spectral studies on the Schiff base mode of all-*trans* bacteriorhodopsin and its photointermediates, K and L. *Photochem. Photobiol.* **54**, 911-921
- Sasaki, J., Yuzawa, T., Kandori, H., Maeda, A., and Hamaguchi,

- H. (1995) Nanosecond time-resolved infrared spectroscopy distinguishes two K species in the bacteriorhodopsin. *Biophys. J.* **68**, 2073-2080
14. Sasaki, J., Maeda, A., Kato, C., and Hamaguchi, H. (1993) Time-resolved infrared spectral analysis of the KL-to-L conversion in the photocycle of bacteriorhodopsin. *Biochemistry* **32**, 867-871
 15. Maeda, A., Sasaki, J., Shichida, Y., and Yoshizawa, T. (1992) Water structure changes in bacteriorhodopsin photocycle: Analysis by Fourier transform infrared spectroscopy. *Biochemistry* **31**, 462-467
 16. Kandori, H., Yamazaki, Y., Sasaki, J., Needleman, R., Lanyi, J.K., and Maeda, A. (1995) Water-mediated proton transfer in proteins: An FTIR study of bacteriorhodopsin. *J. Am. Chem. Soc.* **117**, 2118-2119
 17. Scheiner, S. and Duan, X. (1991) Effect of intermolecular orientation upon proton transfer within a polarizable medium. *Biophys. J.* **60**, 874-883
 18. Brown, L.S., Gat, Y., Sheves, M., Yamazaki, Y., Maeda, A., Needleman, R., and Lanyi, J.K. (1994) The retinal Schiff base-counterion complex of bacteriorhodopsin: Changed geometry during the photocycle is a cause of proton transfer to aspartate 85. *Biochemistry* **33**, 12001-12011
 19. Brown, L.S. and Lanyi, J.K. (1996) Determination of the transiently lowered pK_a of the retinal Schiff base during the photocycle of bacteriorhodopsin. *Proc. Natl. Acad. Sci. USA* **93**, 1731-1734
 20. Humphrey, W., Xu, D., Sheves, M., and Schulten, K. (1995) Molecular dynamics study of the early intermediates in the bacteriorhodopsin photocycle. *J. Phys. Chem.* **99**, 14549-14560
 21. Xu, D., Sheves, M., and Schulten, K. (1995) Molecular dynamics study of the M_{412} intermediate of bacteriorhodopsin. *Biophys. J.* **69**, 2745-2760
 22. Chon, Y.-S., Sasaki, J., Kandori, H., Brown, L.S., Lanyi, J.K., Needleman, R., and Maeda, A. (1996) Hydration of the counterion of the Schiff base in the chloride transporting mutant of bacteriorhodopsin: FTIR and FT-Raman studies on the effects of anion binding when Asp85 is replaced with a neutral residue. *Biochemistry* **35**, 14244-14250
 23. Sasaki, J., Brown, L.S., Chon, Y.-S., Kandori, H., Maeda, A., Needleman, R., and Lanyi, J.K. (1995) Conversion of bacteriorhodopsin into a chloride ion pump. *Science* **269**, 73-75
 24. Blanck, A. and Oesterheld, D. (1987) The halo-opsin gene II. Sequence, primary structure of halorhodopsin and comparison with bacteriorhodopsin. *EMBO J.* **6**, 265-273
 25. Váró, G., Brown, L.S., Sasaki, J., Kandori, H., Maeda, A., Needleman, R., and Lanyi, J.K. (1995) Light-driven chloride ion transport by halorhodopsin from *Natronbacterium pharaonis*. 1. The photochemical cycle. *Biochemistry* **34**, 14490-14499
 26. Váró, G., Needleman, R., and Lanyi, J.K. (1995) Light-driven chloride ion transport by halorhodopsin from *Natronbacterium pharaonis*. 2. Chloride release and uptake, protein conformation change, and thermodynamics. *Biochemistry* **34**, 14500-14507
 27. Braiman, M.S., Walther, T.J., and Biercheck, D.M. (1994) Infrared spectroscopic detection of light-induced change in chloride-arginine interaction in halorhodopsin. *Biochemistry* **33**, 1629-1723
 28. Braiman, M.S., Mogi, T., Marti, T., Stern, L.J., Khorana, H.G., and Rothschild, K.J. (1988) Vibrational spectroscopy of bacteriorhodopsin mutants: light-driven proton transport involves protonation changes of aspartic acid residues 85, 96 and 212. *Biochemistry* **27**, 8516-8520
 29. Maeda, A., Sasaki, J., Shichida, Y., and Yoshizawa, T., Chang, M., Ni, B., Needleman, R., and Lanyi, J.K. (1992) Structures of aspartic acid-96 in the L and N intermediates of bacteriorhodopsin: Analysis by Fourier transform infrared spectra. *Biochemistry* **31**, 4684-4690
 30. Yamazaki, Y., Hatanaka, M., Kandori, H., Sasaki, J., Karstens, J., Raap, J., Lugtenburg, J., Bizounok, M., Herzfeld, J., Needleman, R., Lanyi, J.K., and Maeda, A. (1995) Water structural changes at the proton uptake site (the Thr46-Asp96 domain) in the L intermediate of bacteriorhodopsin. *Biochemistry* **34**, 7088-7093
 31. Yamazaki, Y., Tuzi, S., Saito, H., Kandori, H., Needleman, R., Lanyi, J.K., and Maeda, A. (1996) Hydrogen-bonds of water and C-O groups coordinate long-range structural changes in the L photointermediate of bacteriorhodopsin. *Biochemistry* **35**, 4063-4068
 32. Ludlam, C.F.C., Sonar, S., Lee, C.-P., Coleman, M., Herzfeld, J., RajBhandary, U.L., and Rothschild, K.J. (1995) Site-directed isotope labelling and ATR-FTIR difference spectroscopy of bacteriorhodopsin: the peptide carbonyl group of TYR185 is structurally active during the bR→N transition. *Biochemistry* **34**, 2-6
 33. Richter, H.-T., Brown, L.S., Needleman, R., and Lanyi, J.K. (1996) A linkage of the pK_a 's of asp-85 and glu-204 forms part of the reprotonation switch of bacteriorhodopsin. *Biochemistry* **35**, 4054-4062
 34. Sasaki, J., Lanyi, J.K., Needleman, R., Yoshizawa, T., and Maeda, A. (1994) Complete identification of C-O stretching vibrational bands of protonated aspartic acid residues in the difference infrared spectra of M and N intermediates versus bacteriorhodopsin. *Biochemistry* **33**, 3178-3184
 35. Maeda, A., Sasaki, J., Ohkita, Y.J., Simpson, M., and Herzfeld, J. (1992) Tryptophan perturbation in the L intermediate of bacteriorhodopsin: Fourier transform infrared analysis with indole- ^{15}N shift. *Biochemistry* **31**, 12543-12545
 36. Yamazaki, Y., Sasaki, J., Hatanaka, M., Kandori, H., Maeda, A., Needleman, R., Shinada, T., Yoshihara, K., Brown, L.S., and Lanyi, J.K. (1995) Interaction of tryptophan-182 with the retinal 9-methyl group in the L intermediate of bacteriorhodopsin. *Biochemistry* **34**, 577-582
 37. Kamikubo, H., Kataoka, M., Váró, G., Oka, T., Tokunaga, F., Needleman, R., and Lanyi, J.K. (1996) Structure of the N intermediate of bacteriorhodopsin revealed by X-ray diffraction. *Proc. Natl. Acad. Sci. USA* **93**, 1386-1390
 38. Cao, Y., Brown, L.S., Sasaki, J., Maeda, A., Needleman, R., and Lanyi, J.K. (1995) Relationship of proton release at the extracellular surface to deprotonation of the Schiff base in the bacteriorhodopsin photocycle. *Biophys. J.* **68**, 1518-1530
 39. Brown, L.S., Sasaki, J., Kandori, H., Maeda, A., Needleman, R., and Lanyi, J.K. (1995) Glutamic acid-204 is the terminal proton release group at the extracellular surface of bacteriorhodopsin. *J. Biol. Chem.* **270**, 27122-27126
 40. Otto, H., Marti, T., Holz, M., Mogi, T., Stern, L., Engel, F., Khorana, H.G., and Heyn, M.P. (1990) *Proc. Natl. Acad. Sci. USA* **87**, 1018-1022
 41. Brown, L.S., Váró, G., Hatanaka, M., Sasaki, J., Kandori, H., Maeda, A., Friedman, N., Sheves, J., Needleman, R., and Lanyi, J.K. (1995) The complex extracellular domain regulates the deprotonation and reprotonation of the retinal Schiff base during the bacteriorhodopsin photocycle. *Biochemistry* **34**, 12903-12911
 42. Govindjee, R., Misra, S., Balashov, S.P., Ebrey, T.G., Crouch, R.K., and Menick, D.R. (1996) Arginine-82 regulates the pK_a of the group responsible for the light-driven proton release in bacteriorhodopsin. *Biophys. J.* **71**, 1011-1023
 43. Hatanaka, M., Sasaki, J., Kandori, H., Ebrey, T.G., Needleman, R., Lanyi, J.K., and Maeda, A. (1996) Effects of arginine-82 on the interactions of internal water molecules in bacteriorhodopsin. *Biochemistry* **35**, 6308-6312
 44. Otto, H., Marti, T., Holz, M., Mogi, T., Lindau, M., Khorana, H.G., and Heyn, M.P. (1989) Aspartic acid-96 is the internal proton donor in the reprotonation of the Schiff base of bacteriorhodopsin. *Proc. Natl. Acad. Sci. USA* **86**, 9228-9232
 45. Sasaki, J., Shichida, Y., Lanyi, J.K., and Maeda, A. (1992) Protein changes associated with reprotonation of the Schiff base in the photocycle of Asp⁸⁵→Asn bacteriorhodopsin: The M_N intermediate with unprotonated Schiff base but N-like protein structure. *J. Biol. Chem.* **267**, 20782-20786
 46. Kataoka, M., Kamikubo, H., Tokunaga, F., Brown, L.S., Yamazaki, Y., Maeda, A., Sheves, M., Needleman, R., and Lanyi, J.K. (1994) Energy coupling in an ion pump: the reprotonation switch of bacteriorhodopsin. *J. Mol. Biol.* **243**, 621-638
 47. Brown, L.S., Yamazaki, Y., Maeda, A., Sun, L., Needleman, R.,

- and Lanyi, J.K. (1994) The proton transfers in the cytoplasmic domain of bacteriorhodopsin are facilitated by a cluster of interacting residues. *J. Mol. Biol.* **239**, 401-414
48. Riesle, J., Oesterhelt, D., Dencher, N.A., and Heberlé, J. (1996) D38 is an essential part of the proton translocation pathway in bacteriorhodopsin. *Biochemistry* **35**, 6635-6643
49. Smith, S.O., Pardo, J.A., Mulder, P.P.J., Curry, B., Lugtenburg, J., and Mathies, R.A. (1983) Chromophore structure of bacteriorhodopsin's O₆₄₀ photointermediate. *Biochemistry* **22**, 6141-6148
50. Richter, H.-T., Needleman, R., Kandori, H., Maeda, A., and Lanyi, J.K. (1996) Relationship of retinal configuration and internal proton transfer at the end of the bacteriorhodopsin photocycle. *Biochemistry* **35**, 15461-15466
51. Jäger, F., Fahmy, K., Sakmar, T.P., and Siebert, F. (1994) Identification of glutamic acid-113 as the Schiff base proton acceptor in the metarhodopsin II photointermediate of rhodopsin. *Biochemistry* **33**, 10878-10882
52. Arnis, S., Fahmy, K., Hofmann, P.K., and Sakmar, T.P. (1994) A conserved carboxylic acid group mediates light-dependent proton uptake and signaling by rhodopsin. *J. Biol. Chem.* **269**, 23879-23881
53. Arnis, S.M. and Hofmann, K.P. (1993) Two different forms of metarhodopsin II: Schiff base deprotonation precedes proton uptake and signaling state. *Proc. Natl. Acad. Sci. USA* **90**, 7849-7853
54. Palings, I., van den Berg, E.M.M., Lugtenburg, J., and Mathies, R.A. (1989) Complete assignment of the hydrogen out-of-plane wagging vibrations of bathorhodopsin: chromophore structure and energy storage in the primary photoproduct of vision. *Biochemistry* **28**, 1498-1507
55. Sasaki, J., Maeda, A., Shichida, Y., Groesbeek, M., Lugtenburg, J., and Yoshizawa, T. (1992) Structure of hypsorhodopsin: Analysis by Fourier transform infrared spectroscopy at 10 K. *Photochem. Photobiol.* **56**, 1063-1071
56. Ohkita, Y.J., Sasaki, J., Maeda, A., Yoshizawa, T., Groesbeek, M., Verdegem, P., and Lugtenburg, J. (1995) Changes in structure of the chromophore in the photochemical process of bovine rhodopsin as revealed by FTIR spectroscopy for hydrogen-out-of-plane vibrations. *Biophys. Chem.* **56**, 71-78
57. Nishimura, S., Kandori, H., Nakagawa, M., Tsuda, M., and Maeda, A. (1996) Structural dynamics of water and the peptide backbone around the Schiff base associated with the light-activated process of octopus rhodopsin. *Biochemistry* **36**, 864-870
58. Terakita, A., Hariyama, T., Tsukahara, Y., Katsukura, Y., and Tashiro, H. (1993) Interaction of GTP-binding protein Gq with photoactivated rhodopsin in the photoreceptor membrane of crayfish. *FEBS Lett.* **330**, 197-200
59. Kandori, H. and Maeda, A. (1995) FTIR spectroscopy reveals microscopic structural changes of the protein around the rhodopsin chromophore upon photoisomerization. *Biochemistry* **34**, 14220-14229
60. Maeda, A., Ohkita, Y.J., Sasaki, J., Shichida, Y., and Yoshizawa, T. (1993) Water structural changes in lumirhodopsin, metarhodopsin I, and metarhodopsin II upon photolysis of bovine rhodopsin: Analysis by Fourier transform infrared spectroscopy. *Biochemistry* **32**, 12033-12038
61. Nishimura, S., Sasaki, J., Kandori, H., Lugtenburg, J., and Maeda, A. (1995) Structural changes in the lumirhodopsin-to-metarhodopsin I conversion of air-dried bovine rhodopsin. *Biochemistry* **34**, 16758-16763
62. Nishimura, S., Sasaki, J., Kandori, H., Matsuda, T., Fukada, Y., and Maeda, A. (1996) Structural changes in the peptide backbone in complex formation between activated rhodopsin and transducin studied by FTIR spectroscopy. *Biochemistry* **35**, 13267-13271